Chemistry—Methods

Research Article
doi.org/10.1002/cmtd.202200075

Chemistry Europe
European Chemical Societies Publishing

www.chemistrymethods.org

^{13}C and ^{15}N Benchtop NMR Detection of Metabolites via Relayed Hyperpolarization**

Seyma Alcicek,*[a, b] Erik Van Dyke,[c] Jingyan Xu,[c] Szymon Pustelny,[a] and Danila A. Barskiy*[c]

Parahydrogen-based nuclear spin hyperpolarization allows various magnetic-resonance applications, and it is particularly attractive because of its technical simplicity, low cost, and ability to quickly (in seconds) produce large volumes of hyperpolarized material. Although many parahydrogen-based techniques have emerged, some of them remain unexplored due to the lack of careful optimization studies. In this work, we investigate and optimize a novel parahydrogen-induced polarization (PHIP) technique that relies on proton exchange referred to below as PHIP-relay. An INEPT (insensitive nuclei enhanced by polarization transfer) sequence is employed to transfer polarization from hyperpolarized protons to heteronuclei (^{15}N and ^{13}C) and nuclear signals are detected using benchtop NMR spectrometers (1 T and 1.4 T, respectively). We demonstrate the applicability of the PHIP-relay technique for hyperpolarization of a wide range of biochemicals by examining such key metabolites as urea, ammonium, glucose, amino acid glycine, and a drug precursor benzamide. By optimizing chemical and NMR parameters of the PHIP-relay, we achieve a 17,100-fold enhancement of ^{15}N signal of [^{13}C, $^{15}N_2$]-urea compared to the thermal signal measured at 1 T. We also show that repeated measurements with shorter exposure to parahydrogen provide a higher effective signal-to-noise ratio compared to longer parahydrogen bubbling.

Introduction

Magnetic resonance (MR) is an extremely rich physical phenomenon as it is widely used in many areas of modern science and technology including chemical analysis and medical diagnostics.[1–3] However, the widespread applicability of the technique is hindered by the inherently poor sensitivity of NMR, originating from very low spin polarization despite the use of often expensive and bulky superconducting magnets.[4–7] This problem has led to the development of various hyperpolarization approaches that produce non-equilibrium nuclear polarization by sample manipulation.[8] As a result, many unexplored applications of MR are becoming possible. For example, it has been shown that the use of ^{15}N-labelled probes for molecular imaging enables higher spatial resolutions. This is due to the absence of quadrupolar ^{14}N nuclei, which accelerate T_2 relaxation of neighboring ^{13}C nuclei at high fields.[9–11] Molecular imaging of hyperpolarized metabolites to explore the complex microenvironment of abnormal tissues would provide crucial information for the early diagnosis, treatment and prognosis of a disease.[12–16] Furthermore, hyperpolarization of highly biocompatible endogenous imaging probes, such as urea, holds great promise for MR angiography and perfusion imaging.[17–21]

Besides urea, there are other N-containing small biomolecules which could be of interest in the molecular imaging field, such as glycine, an amino acid and precursor of many important proteins (e.g., glutathione, creatine, hemoprotein, etc.). In addition to the key role of glycine in many metabolic pathways as a neurotransmitter, cryoprotector, and immuno-modulator, a significant impact of its metabolism on cancer cell proliferation has been reported.[22,23] Another example is ammonium, a metabolite produced by catabolism of compounds containing nitrogen, such as amino acids.[24] An increase in ammonium levels in the human body is mainly the result of disorders in the liver, kidneys, or stomach, and its real-time *in vivo* detection has been an attractive topic for clinical care.[25] Apart from medicine, ammonia has also been investigated as a carbon-free energy carrier and storage material.[26] As a final example, benzamide can be given, a precursor of many drugs in clinical use.[27]

Thus far, the leading technique used in clinical studies for the production of hyperpolarized molecules has been dissolution dynamic nuclear polarization (*d*DNP).[28,29] Parahydrogen-(pH_2)-based methods could be advantageous over *d*DNP for certain applications due to their low cost, technical simplicity, and ability to rapidly and continuously produce large volumes of hyperpolarized material.[4,30,31] Additionally, integration of such techniques with portable benchtop NMR spectrometers promises the democratization of NMR equipment and improvement of its sensitivity. One of the drawbacks of hydrogenative

[a] Dr. S. Alcicek, Prof. S. Pustelny
Institute of Physics, Faculty of Physics, Astronomy and Applied Computer Science, Jagiellonian University in Kraków, 30-348 Kraków, Poland
E-mail: seyma.alcicek@kgu.de
[b] Dr. S. Alcicek
Institute of Neuroradiology, University Hospital Frankfurt, Goethe University, 60528, Frankfurt am Main, Germany
E-mail: seyma.alcicek@kgu.de
[c] E. Van Dyke, J. Xu, Dr. D. A. Barskiy
Helmholtz Institute Mainz, GSI Helmholtz Center for Heavy Ion Research GmbH, 55128 Mainz, Germany
and
Institute of Physics, Johannes Gutenberg-Universität, 55128 Mainz, Germany
E-mail: dbarskiy@uni-mainz.de

[**] A previous version of this manuscript has been deposited on a preprint server (https://doi.org/10.26434/chemrxiv-2022-vzr8f).

Supporting information for this article is available on the WWW under https://doi.org/10.1002/cmtd.202200075

Research Article
doi.org/10.1002/cmtd.202200075

Chemistry Europe
European Chemical Societies Publishing

parahydrogen-induced polarization (PHIP) is the need for a dedicated compound (precursor) that is chemically modified during the reaction to produce a hyperpolarized target molecule.[32–34] Recently, this problem has been addressed through the development of SABRE-relay (SABRE = signal amplification by reversible exchange) and PHIP-relay (also introduced in the literature as PHIP-X), both employing proton exchange to transmit hyperpolarization from a transfer agent to a second – and potentially subsequent – molecular target.[35,36] These approaches have extended the applicability of PHIP (ALTADENA) toward hyperpolarization of a wide range of biomolecules possessing exchangeable protons such that a target molecule is not chemically altered during the *brutto* chemical process. In the original work,[36] PHIP-relay was used to hyperpolarize biomolecules with –OH groups such as pyruvic and lactic acids, D-[$^{13}C_6$]-glucose, achieving maximum ^{1}H polarization level of 0.07 % on the target molecule, while polarization level of 13 % was reported in a transfer molecule. This shows that even though PHIP-relay is an attractive hyperpolarization method, optimization studies are generally required for an efficient transfer of polarization to the molecule of interest.

Here, we implement the PHIP-relay technique on (bio)-molecules with a substantial improvement of its efficiency. This study is carried out using benchtop NMR spectrometers (1 T and 1.4 T) combined with a robotic arm setup for pH_2 delivery and magnetic field control, which allowed automated optimization of experimental parameters. Allyl alcohol (produced from propargyl alcohol) is used as a hyperpolarized carrier molecule for a subsequent polarization transfer via the proton-exchange mechanism at low magnetic fields.[36,37] In allyl alcohol molecules, all protons interact strongly and magnetization can be distributed throughout all coupled ^{1}H spins in the absence of heteronuclei.[32,35,36,38] To maximize the efficiency of polarization transfer, key parameters such as catalyst concentration, pH_2 bubbling time, polarization transfer field, and transfer time have been studied. A well-known NMR pulse sequence INEPT (insensitive nuclei enhanced by polarization transfer) was used to enhance the ^{15}N NMR signal of hyperpolarized target molecules: [$^{15}N_2$]-urea, [^{13}C, $^{15}N_2$]-urea, [^{15}N]-glycine, [^{15}N]-ammonium nitrate, and [^{15}N]-benzamide. In addition, D-[1-^{13}C]-glucose was hyperpolarized via PHIP-relay and detected using ^{1}H-^{13}C INEPT NMR spectroscopy at 1.4 T.

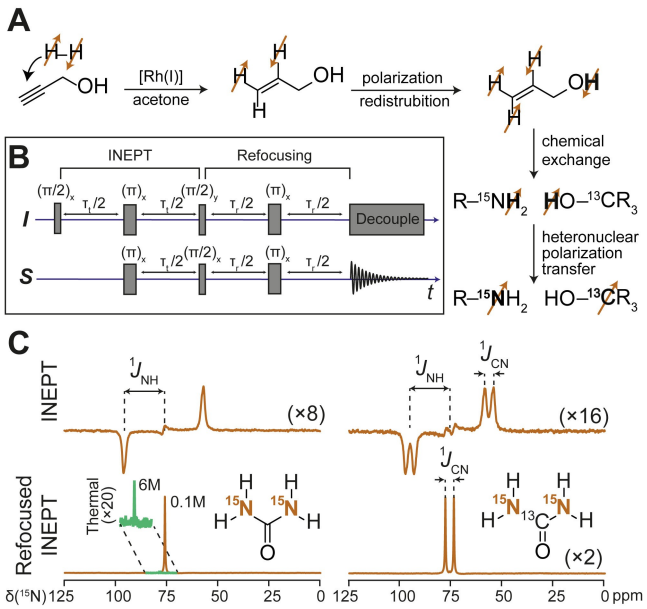

Figure 1. (A) Schematic representation of the PHIP-relay process; (B) Basic and refocused INEPT pulse sequences. Transfer and refocusing spin-echo time intervals are denoted as $\tau_t/2$ and $\tau_t/2$, respectively. (C) Basic and refocused (with ^{1}H decoupling) single scan ^{1}H-^{15}N INEPT NMR spectra of 0.1 M [$^{15}N_2$]-urea (top) and 0.1 M [^{13}C, $^{15}N_2$]-urea (bottom) hyperpolarized via PHIP-relay. Green trace shows INEPT spectrum of a thermally polarized ^{15}N-ammonium (6 M) for comparison.

Results and Discussion

PHIP-relay can be described as a two-stage process (we emphasize that nomenclature PHIP-relay is used in this work to highlight that chemical relay is a crucial stage of the process in analogy with SABRE-relay; the first demonstration, however, was dubbed PHIP-X which creates potential confusion with X-SABRE[39]). Initially, a transfer molecule, e.g., allyl alcohol, is hyperpolarized by adding pH_2 to an unsaturated carbon-carbon bond of propargyl alcohol. Then, polarization is transferred from the hyperpolarized transfer molecule (e.g., hyperpolarized allyl alcohol) to a target molecule via the proton-exchange (Figure 1A). The first step, which is the well-known PHIP-ALTADENA experiment[40] (adiabatic longitudinal transport after dissociation engenders net alignment) in which hydrogenation at low field followed by adiabatic passage to high field for detection, has a significant effect on the target-compound hyperpolarization. Thus, the efficiency of the propargyl alcohol hydrogenation reaction with pH_2 to hyperpolarize allyl alcohol and then propanol was studied for various amounts of Rh(I)-catalyst (5, 10, 15 mM) and different pH_2 bubbling times.

As shown in the Supporting Information, the highest amount of the catalyst induced the fastest consumption of propargyl and allyl alcohol (Figure S1B). In the experiments with 5 mM catalyst, propanol production was observed after 40 s of hydrogen bubbling, while for a catalyst concentration of 10 mM, propanol appeared in the solution after 20–30 s of bubbling with hydrogen. As the gradual production of allyl alcohol allows acquiring many NMR transients, thus, prolonging a measurement time per sample, 5 mM catalyst was used in further experiments. Furthermore, allyl alcohol had the highest polarization after 20–30 s bubbling, and propanol became a primary source of polarization after 50–60 s of exposure to pH_2. However, during the first 60 s of bubbling, the polarization level of propanol was never as high as the maximum polarization of allyl alcohol. Therefore, even though propanol could also be considered as a transfer agent for the PHIP-relay technique, allyl alcohol seems to be more suitable for high-polarization transfer to a target molecule.

As the next step, the polarization transfer to a target molecule was investigated. Due to the complexity of the ^{1}H NMR spectrum, with many peaks originating from the transfer

Research Article
doi.org/10.1002/cmtd.202200075
Chemistry Europe
European Chemical Societies Publishing

and target compounds, the ^{1}H-^{15}N and ^{1}H-^{13}C INEPT techniques were used to facilitate spectral analysis. INEPT is a specific pulse sequence used in NMR to enhance signal resolution by transferring polarization from coupled protons (here hyperpolarized protons via PHIP-relay) to a heteronucleus.[41] While the basic INEPT sequence generates anti-phase magnetization, additional spin echo sandwich (Figure 1B) in the refocused INEPT sequence produces in-phase magnetization.[42] Decoupling was applied following the refocused INEPT sequence to obtain in-phase heteronuclear NMR signals. Optimal spin-echo delays for the INEPT pulse sequence for each molecule were calculated based on numerical simulations (see Supporting Information for details).

Figure 1C shows the single-transient basic and refocused ^{1}H-^{15}N INEPT spectra of [^{13}C, ^{15}N$_2$]-urea and [^{15}N$_2$]-urea hyperpolarized via PHIP-relay. NMR samples (0.5 M propargyl alcohol, 5 mM Rh(I)-catalyst, 100 mM urea in DMSO and acetone mixture) were bubbled with pH$_2$ at the Earth's magnetic field for 20 s before acquiring the ^{15}N NMR spectra. As expected, in the spectra of [^{15}N$_2$]-urea subjected to the refocused INEPT (with proton decoupling), a single line appears at ≈75 ppm, while in the basic INEPT spectrum (without proton decoupling), the line is split by J_{NH}-coupling. The existence of an additional ^{13}C-^{15}N J-coupling interaction in [^{13}C, ^{15}N$_2$]-urea results in further splitting of the peaks into doublets, which carries half of the signal intensity. Narrower lines in the refocused INEPT spectra compared to those of the basic INEPT spectra result from decoupling which eliminates the effect of proton exchange on line broadening.

After hyperpolarizing urea via PHIP-relay, optimization of the bubbling field (0.05–80 mT) and bubbling time (5–120 s) was performed. To study the influence of the pH$_2$ bubbling time on signal enhancement, four identical NMR samples (0.5 M propargyl alcohol, 5 mM Rh(I)-catalyst, 100 mM [^{13}C, ^{15}N$_2$]-urea dissolved in DMSO and acetone mixture) were prepared. For each bubbling time interval (5, 20, 40, and 60 s), one of the samples was bubbled with pH$_2$ in the Earth's field and then the NMR tube was transferred into the spectrometer via robotic arm to obtain the ^{1}H-^{15}N refocused INEPT NMR spectrum of hyperpolarized [^{13}C, ^{15}N$_2$]-urea. This process was repeated for each sample 24, 6, 3, and 2 times for the corresponding bubbling time (total bubbling time is the same for all samples). Owing to the high concentration of the primary substrate (i.e. here propargyl alcohol, the production of hyperpolarized transfer agents continues for many transients, allowing repolarization of the target molecule. This approach enabled us to acquire many NMR signals originating from the repolarized target molecule, as shown in Figure 2A. The highest signal enhancement in a single scan is observed after 60 s of bubbling, when allyl alcohol and propanol had almost the same polarization level (Figure S1C). This may lead to the conclusion that the effect of propanol as a transfer agent is not insignificant. Although the long bubbling time appears to be more efficient per scan, the accumulated spectra from repeated measurements show that PHIP-relay with short bubbling time can provide an overall higher signal-to-noise ratio per pH$_2$ bubbling duration (Figure 2B).

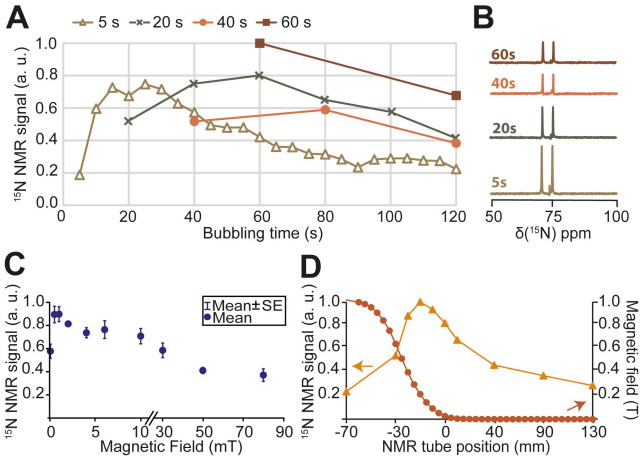

Figure 2. (A) Effect of pH$_2$ bubbling time on the ^{1}H-^{15}N INEPT NMR signal of hyperpolarized [^{13}C, ^{15}N$_2$]-urea. The graph corresponds to four NMR samples of urea which were bubbled with pH$_2$ several times (24, 6, 3, and 2) in different time intervals (5, 20, 40, and 60 s, respectively). (B) Accumulated ^{1}H-^{15}N refocused INEPT NMR spectra of hyperpolarized [^{13}C, ^{15}N$_2$]-urea for each bubbling time interval. Signal-to-noise ratio values for urea peaks are estimated as 37, 32, 62, 102 (from top to bottom, respectively). (C) The magnetic field (0.05–80 mT) dependence of the ^{15}N NMR signal enhancement of [^{13}C, ^{15}N$_2$]-urea. Each data point is a result of averaged three transients after repeated 20 s of the pH$_2$ supply, error bars represent standard deviations. (D) Intensity of hyperpolarized [^{13}C, ^{15}N$_2$]-urea signal versus the position of NMR tube inside the bore of the spectrometer during PHIP-relay. Each data point corresponds to a measurement following a transfer of the sample into the detection region after 10 s of pH$_2$ bubbling in a given position. Magnetic field profile was measured using a gaussmeter. The location of the tube was determined based on "0" position of the robotic arm (see Supporting Information).

In order to investigate the influence of the pH$_2$ bubbling field on the signal enhancement, ten different magnetic fields were selected between the Earth's field and 80 mT. In each field, the NMR samples (0.5 M propargyl alcohol, 5 mM Rh(I)-catalyst, 100 mM [^{13}C, ^{15}N$_2$]-urea in DMSO and acetone mixture) were exposed to pH$_2$ for 20 s. Immediately after bubbling, the sample was transferred with a robotic arm to the benchtop NMR spectrometer to record the refocused ^{1}H-^{15}N INEPT NMR spectrum. For each sample, the measurement was repeated three times; the resultant mean values and standard deviations of the relative signals are presented in Figure 2C. When the bubbling field was around 2 mT, the highest signal enhancement was observed. Increasing the magnetic field to 80 mT resulted in a gradual decrease of signal intensity. Numerical simulations published previously[36] showed that increase of the magnetic field up to 80 mT during hydrogenation should result in the significant increase of the –OH group's NMR signal. Our experimental results refute this conclusion. However, polarization redistribution during the sample transfer as well as polarization transfer from the –OH group of the transfer molecule to the target molecule (the key step that can also be influenced by the magnetic field strength) can complicate theoretical analysis. Further studies are necessary for explaining the disagreement between our experimental data and simulations conducted to date.

Even though hyperpolarization of the target molecule via PHIP-relay is more efficient when a low magnetic field is applied

Research Article
doi.org/10.1002/cmtd.202200075
Chemistry Europe
European Chemical Societies Publishing

during hydrogenation with pH_2, relaxation throughout the transfer (taking approximately 3 s) significantly lowers the signal intensity. For this reason, we took advantage of the magnetic field inside the bore of the $^1H/^{15}N$ NMR spectrometer, where the field varied from the Earth's field to 1 T. By changing the sample position inside the bore of the spectrometer, we performed hydrogenation with pH_2 at varying bubbling field, thus, shortening transfer time. An NMR sample (0.5 M of propargyl alcohol, 5 mM of Rh(I)-catalyst, of 100 mM [^{13}C, $^{15}N_2$]-urea dissolved in the DMSO and acetone mixture) was exposed to pH_2 for 10 s in a given location inside the bore and, subsequently, it was moved to the detection region by the robotic arm to acquire refocused ^1H-^{15}N INEPT NMR spectrum. This experiment was repeated for ten different locations inside the bore (Figure 2D). When the NMR tube was in the middle of the magnet bore (≈0.2 T) during hydrogenation with pH_2, a single-scan enhancement of ≈17,100 was observed for [^{13}C, $^{15}N_2$]-urea. This corresponded to a polarization level of 1.2% per molecule. Such a large signal was detected due to the short transfer time which reduces relaxation losses in the course of the sample transfer. When the sample was hydrogenated with pH_2 at a magnetic field closer to the Earth's field or high field (1 T), the decrease in signal intensity was observed. By taking into account the effect of the differences in the sample transfer times for each measurement, these observations are congruent with the previous result concerning optimization of the applied magnetic field during hydrogenation with pH_2.

As the next step, samples of 15 mM [^{15}N]-glycine, 50 mM [^{15}N]-ammonium and 50 mM [^{15}N]-benzamide in the DMSO and acetone mixtures were prepared with additional 0.5 M propargyl alcohol and 5 mM Rh(I)-catalyst. Each sample was subjected to pH_2 bubbling for 20 s in the Earth's field and transferred to the spectrometer to obtain the refocused ^1H-^{15}N INEPT NMR spectra of hyperpolarized ^{15}N-labelled compounds. Spin-echo delays for INEPT experiments were calculated using numerical simulations (see Supporting Information for details). Peaks in the spectra of [^{15}N]-glycine, [^{15}N]-ammonium, and [^{15}N]-benzamide were observed with a few orders of magnitude signal enhancement, namely, corresponding to 0.1%, 0.13% and 0.02% ^{15}N polarization levels per molecule, respectively (Figure 3A). It is important to note that the polarization levels could be further improved by performing experiments in the optimum bubbling field, even more so by shortening the transfer time as mentioned above.

Finally, hyperpolarization of D-[1-^{13}C]-glucose is reported showing the feasibility of using PHIP-relay methodology combined with ^1H-^{13}C INEPT pulse sequence for ^{13}C NMR signal enhancement of carbohydrates. Unlike crowded ^1H NMR spectra with numerous peaks originating from the hyperpolarized protons of transfer and target compounds, ^{13}C NMR detection endows clear discrimination of the chemicals. For this purpose, pH_2 gas was bubbled through a sample containing 60 mM D-[1-^{13}C]-glucose, 0.5 M propargyl alcohol, and 5 mM Rh(I)-catalyst dissolved in the mixtures of DMSO and acetone at the Earth's field. Immediately after bubbling, the NMR tube was transferred to the ^1H-^{13}C NMR spectrometer for acquiring the refocused ^1H-^{13}C INEPT NMR spectrum. In order to assign the peaks arising

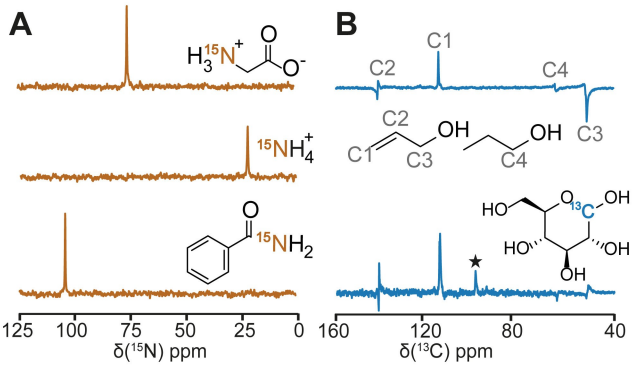

Figure 3. (A) Single scan refocused ^1H-^{15}N INEPT NMR spectra of hyperpolarized [^{15}N]-glycine, [^{15}N]-ammonium, and [^{15}N]-benzamide via PHIP-relay. (B) Refocused ^1H-^{13}C INEPT NMR spectrum of hyperpolarized products: allyl alcohol and propanol (above) and refocused single-scan ^1H-^{13}C INEPT NMR spectrum of D-[1-^{13}C]-glucose hyperpolarized via PHIP-relay. The peak at ≈100 ppm (denoted with star) originates from D-[1-^{13}C]-glucose.

from the naturally abundant ^{13}C isotope in hyperpolarized allyl alcohol and propanol, a PHIP solution consisting of the chemicals listed above, except for D-[1-^{13}C]-glucose, was measured in the same way. Top spectrum in Figure 3B is the result of an experiment with the mentioned solution without D-[1-^{13} C]-glucose, while the bottom spectrum is the experiment with a sample containing D-[1-^{13}C]-glucose. The peak associated with hyperpolarized D-[1-^{13}C]-glucose arose at about 100 ppm (estimated signal intensity corresponds to 0.024% ^{13}C polarization) while the other peaks originate from hyperpolarized allyl alcohol and propanol.

Besides the achievement of a substantial increment (a 17,100-fold) in urea signal after optimization studies (sample composition, pH_2 exposure time, magnetic field during hydrogenation, sample transfer time, etc.) presented above, other important N-containing molecules were used to demonstrate the potential of PHIP-relay for the hyperpolarization of a wide range of chemicals. As shown above, NMR signals of these molecules were boosted significantly, albeit to a lesser extent than urea.

In hyperpolarized MR spectroscopic imaging (MRSI), the low natural abundance of ^{13}C and ^{15}N nuclei limits the background noise that arises from metabolites based on carbon and nitrogen.[15,43] Although spin-1/2 nuclei with low gyromagnetic ratio (γ) typically display longer longitudinal relaxation times, thus, allowing relatively long measurement times, acquisition of their spectra is a challenge due to the fact that MR signal is proportional to γ using inductive detection.[44] To overcome this challenge, as demonstrated in Refs. [45–47], polarization can be stored on long-lived ^{13}C and ^{15}N nuclei and transferred back to protons for sensitive ^1H NMR detection, prolonging the lifetime of hyperpolarized contrast agents.

Up to now, the proton exchange-based hyperpolarization method SABRE-relay has been used to hyperpolarize [^{13}C, $^{15}N_2$]-urea and [^{13}C]-urea. This method was shown to produce two orders of magnitude signal enhancement for urea compared to the thermal equilibrium polarization measured at 9.4 T[35] (compared to three orders of magnitude demonstrated in the

present study). In addition, SABRE-relay hyperpolarization of [^{13}C]-glucose has been shown to a lesser extent.[35] Despite the lower levels of polarization of bio-molecules obtained via SABRE-relay compared to the results presented here, SABRE-relay has the advantage of allowing re-hyperpolarization and signal accumulation without consuming transfer and target agents, thus improving the signal-to-noise ratio.[30] On the other hand, as reported here, by increasing the amount of a transfer-agent precursor, PHIP-relay can be repeated without full consumption of the target molecule.

Conclusion

In this study, we used a newly developed technique, PHIP-relay, to hyperpolarize biologically relevant metabolites such as urea, amino acids, ammonium, and glucose, as well as a drug precursor benzamide. After sample composition and parameters optimization, we achieved a 17,100-fold enhancement of [^{13}C, $^{15}N_2$]-urea signal through PHIP-relay compared to the thermal signal measured at 1 T, corresponding polarization level of 1.2% per molecule. We also showed that the use of a higher concentration of the transfer agent precursor enables re-hyperpolarization of the target molecule with no change in its structure, thus yielding the acquisition of accumulated signals with a higher signal-to-noise ratio. Despite the fact that the presence of non-biocompatible components (such as organic solvent, catalyst, transfer agent, etc.) is a major challenge for the biomedical translation of the presented technique,[36,48,49] new efficient approaches for sample purification have been recently demonstrated.[50,51] Taken together, the results presented here pave the way for *in vivo* MRSI applications of pH_2-based exchange chemistry coupled with molecule-specific optimization and process automation.

Experimental Methods

All chemicals: propargyl alcohol (CAS# 107-19-7), acetone (CAS# 67-64-1), [^{13}C, $^{15}N_2$]-urea (CAS# 58069-83-3), [$^{15}N_2$]-urea (CAS# 2067-80-3), [^{15}N]-glycine (CAS# 7299-33-4), [^{15}N]-benzamide (CAS# 31656-62-9), [^{15}N]-ammonium nitrate (CAS# 31432-46-9), D-[1-^{13}C]-glucose (CAS# 40762-22-9), and [1,4-Bis-(diphenylphosphino)-butane] (1,5-cyclo-octadiene) rhodium(I) tetrafluoroborate ([Rh(dppb) (COD)]BF_4) (CAS# 79255-71-3) were purchased from MilliporeSigma and used without further purification. NMR measurements were performed using benchtop NMR spectrometers: a SpinSolve Nitrogen ULTRA (40 MHz) and a SpinSolve Carbon (60 MHz), Magritek.

To study hyperpolarization of the transfer agent, solutions of 0.5 M propargyl alcohol and various concentrations of Rh-catalyst (5, 10, 15 mM) were prepared in acetone. For PHIP-relay experiments, 0.5 M propargyl alcohol, 5 mM Rh-catalyst, and the labeled target compound were mixed. Due to the poor solubility of biomolecules in acetone, 50 μL of dimethyl sulfoxide (DMSO) was used for each NMR sample to increase the amount of dissolved molecule of interest. In this way, 100 mM [^{13}C, $^{15}N_2$]-urea and [$^{15}N_2$]-urea; 60 mM D-[1-^{13}C]-glucose; 50 mM [^{15}N]-ammonium nitrate and [^{15}N]-benzamide; and 15 mM [^{15}N]-glycine solutions were prepared.

For each experiment, a 650 μL sample was transferred to a pressurizable 5 mm NMR tube. The NMR tube was then attached to a bubbling system, described in Ref. [37], for pH_2 exposition. Parahydrogen-enriched hydrogen gas was prepared by passing high-purity hydrogen over a hydrated iron(III) oxide catalyst at 30 K using a pH_2 generator (Advanced Research Systems, Inc.). Each NMR sample was bubbled with pH_2 gas through a thin capillary (PTFE, OD: 0.9 mm) for a given time (detailed information is provided below for each experiment). The flow rate of pH_2 was held at 80 sccm at 6 bar using a mass flow controller (Sierra Instruments, Inc.). Subsequent to bubbling with pH_2, the NMR tube was placed in a magnet bore of a benchtop NMR spectrometer using a robotic arm (see Supporting Information, Figure S3). The whole experimental sequence, including the acquisition of NMR signals, was controlled electronically using an Arduino Uno microcontroller board. This automated experimental setup ensures consistency, which is essential to carry out optimization studies with high accuracy. Additionally, using a magnet with adjustable field strength (1–100 mT), various magnetic fields during bubbling were studied to investigate the influence of magnetic field on polarization transfer efficiency through exchangeable protons.

Author Contributions

S.A. and D.A.B. purposed the study. S.A., E.V.D., J.X., and D.A.B. conducted the experiments. S.A. analyzed the results and wrote the initial version of the manuscript. S.P. and D.A.B. contributed to discussion of the experimental results. D.A.B. supervised the overall research effort. All authors edited and finalized the manuscript.

Acknowledgements

S.A. and S.P. acknowledge the support from the European Union's Horizon 2020 research and innovation program under the Marie Skłodowska-Curie grant agreement No. 766402. E.V.D., J.X., and D.A.B. acknowledge the financial support from Alexander von Humboldt Foundation in the framework of the Sofja Kovalevskaja Award. We thank Christopher Suszczynski and Steven Boehmer for providing a sample of [^{13}C, $^{15}N_2$]-urea, Dmitry Budker for providing the access to 1.4 T benchtop NMR spectrometer, and Peter Blümler for the construction of the adjustable magnet capable of generating a variable field in a range of 1 to 101 mT.

Conflict of Interest

The authors declare no conflict of interest.

Data Availability Statement

The data that support the findings of this study are available from the corresponding author upon reasonable request.

Keywords: imaging agents · metabolites · parahydrogen induced polarization (PHIP) · NMR spectroscopy · MRSI

[1] G. F. Pauli, T. Gödecke, B. U. Jaki, D. C. Lankin, *J. Nat. Prod.* **2012**, *75*, 834.
[2] G. A. Nagana Gowda, D. Raftery, *Anal. Chem.* **2017**, *89*, 490.
[3] P. Barker, B. Alberto, R. G. Nicola De Stefano, D. D. M. Lin, *Clinical Mr Spectroscopy : Techniques and Applications.*, Cambridge: Cambridge University Press **2010**.
[4] K. Kovtunov, E. Pokochueva, O. Salnikov, S. Cousin, D. Kurzbach, B. Vuichoud, S. Jannin, E. Chekmenev, B. Goodson, D. Barskiy, I. Koptyug, *Chem. Asian J.* **2018**, *13*, 1857.
[5] D. A. Barskiy, A. M. Coffey, P. Nikolaou, D. M. Mikhaylov, B. M. Goodson, R. T. Branca, G. J. Lu, M. G. Shapiro, V.-V. Telkki, V. V. Zhivonitko, I. V. Koptyug, O. G. Salnikov, K. V. Kovtunov, V. I. Bukhtiyarov, M. S. Rosen, M. J. Barlow, S. Safavi, I. P. Hall, L. Schröder, E. Y. Chekmenev, *Chem. Eur. J.* **2017**, *23*, 725.
[6] P. Nikolaou, B. M. Goodson, E. Y. Chekmenev, *Chem. Eur. J.* **2015**, *21*, 3156.
[7] S. Meier, P. Jensen, M. Karlsson, M. Lerche, *Sensors* **2014**, *14*, 1576 .
[8] J. Eills, D. Budker, S. Cavagnero, E. Y. Chekmenev, S. J. Elliott, S. Jannin, A. Lesage, J. Matysik, T. Meersmann, J. A. R. T. Prisner, H. Yang, I. V. Koptyug, *Chem. Rev.* **2023**, *123*, 1417.
[9] E. Chiavazza, E. Kubala, C. V. Gringeri, S. Düwel, M. Durst, R. F. Schulte, M. I. Menzel, *J. Magn. Reson.* **2013**, *227*, 35.
[10] G. D. Reed, C. von Morze, R. Bok, B. L. Koelsch, M. Van Criekinge, K. J. Smith, H. Shang, P. E. Z. Larson, J. Kurhanewicz, D. B. Vigneron, *IEEE Trans. Med. Imaging* **2014**, *33*, 362.
[11] C. Laustsen, T. Stokholm Nørlinger, D. Christoffer Hansen, H. Qi, P. Mose Nielsen, L. Bonde Bertelsen, J. Henrik Ardenkjaer-Larsen, H. Stødkilde Jørgensen, *Magn. Reson. Med.* **2016**, *75*, 515.
[12] S. Jørgensen, N. Bøgh, E. Hansen, M. Væggemose, H. Wiggers, C. Laustsen, *Semin. Nucl. Med.* **2022**, *52*, 374, Advancement in Instrumentation for Molecular Imaging.
[13] L. M. Le Page, C. Guglielmetti, C. Taglang, M. M. Chaumeil, *Trends Neurosci.* **2020**, *43*, 343.
[14] A. C. Cutter, G. D. Luker, *Radiol. Imaging Cancer* **2019**, *1*, e194001.
[15] Z. J. Wang, M. A. Ohliger, P. E. Z. Larson, J. W. Gordon, R. A. Bok, J. Slater, J. E. Villanueva-Meyer, C. P. Hess, J. Kurhanewicz, D. B. Vigneron, *Radiology* **2019**, *291*, 273.
[16] R. L. Hesketh, K. M. Brindle, *Curr. Opin. Chem. Biol.* **2018**, *45*, 187, Molecular Imaging/Chemical Genetics and Epigenetics.
[17] C. Morze, G. Reed, Z. Wang, M. Ohliger, C. Laustsen, *Methods Mol. Biol.* **2021**, *2216*, 267.
[18] A. Z. Lau, J. J. Miller, M. D. Robson, D. J. Tyler, *Magn. Reson. Med.* **2017**, *77*, 151.
[19] H.-Y. Chen, P. E. Larson, R. A. Bok, C. von Morze, R. Sriram, R. Delos Santos, J. Delos Santos, J. W. Gordon, N. Bahrami, M. Ferrone, J. Kurhanewicz, D. B. Vigneron, *Cancer Res.* **2017**, *77*, 3207.
[20] M. Fuetterer, J. Busch, S. Peereboom, C. Deuster, L. Wissmann, M. Lipiski, T. Fleischmann, N. Cesarovic, C. Stoeck, S. Kozerke, *J. Cardiovasc. Magn. Reson.* **2017**, *19*.
[21] C. von Morze, P. E. Larson, S. Hu, K. Keshari, D. M. Wilson, J. H. Ardenkjaer-Larsen, A. Goga, R. Bok, J. Kurhanewicz, D. B. Vigneron, *J. Magn. Reson. Imaging* **2011**, *33*, 692.
[22] W. Wang, Z. wu, Z. Dai, Y. Yang, J. Wang, G. Wu, *Amino Acids* **2013**, *45*, 463–477.
[23] M. Jain, R. Nilsson, S. Sharma, N. Madhusudhan, T. Kitami, A. L. Souza, R. Kafri, M. W. Kirschner, C. B. Clish, V. K. Mootha, *Science* **2012**, *336*, 1040.
[24] M. M. Adeva, G. Souto, N. Blanco, C. Donapetry, *Metabolism.* **2012**, *61*, 1495.
[25] P. Ricci III, O. Gregory, *Sci. Rep.* **2021**, *11*, 7185.
[26] A. E. Yüzbaşıoğlu, C. Avşar, A. O. Gezerman, *CRGSC* **2022**, *5*, 100307.
[27] W. M. Haynes, D. R. Lide, T. J. Bruno, *CRC Handbook of Chemistry and Physics (97th edition)*, CRC Press/Taylor & Francis **2017**.
[28] J. H. Ardenkjær-Larsen, B. Fridlund, A. Gram, G. Hansson, L. Hansson, M. H. Lerche, R. Servin, M. Thaning, K. Golman, *Proc. Natl. Acad. Sci. USA* **2003**, *100*, 10158.
[29] A. Pinon, A. Capozzi, J. Ardenkjaer-Larsen, *Magn. Reson. Mater. Phys. Biol. Med.* **2020**, *34*, 1.
[30] A. N. Pravdivtsev, G. Buntkowsky, S. B. Duckett, I. V. Koptyug, J.-B. Hövener, *Angew. Chem. Int. Ed.* **2021**, *60*, 23496.
[31] A. B. Schmidt, C. R. Bowers, K. Buckenmaier, E. Y. Chekmenev, H. de Maissin, J. Eills, F. Ellermann, S. Glöggler, J. W. Gordon, S. Knecht, I. V. Koptyug, J. Kuhn, A. N. Pravdivtsev, F. Reineri, T. Theis, K. Them, J.-B. Hövener, *Anal. Chem.* **2022**, *94*, 479.
[32] R. A. Green, R. W. Adams, S. B. Duckett, R. E. Mewis, D. C. Williamson, G. G. Green, *Prog. Nucl. Magn. Reson. Spectrosc.* **2012**, *67*, 1.
[33] L. Buljubasich, M. B. Franzoni, K. Münnemann, *Parahydrogen Induced Polarization by Homogeneous Catalysis: Theory and Applications*, pages 33–74, Springer, Berlin, Heidelberg **2013**.
[34] J. Natterer, J. Bargon, *Prog. Nucl. Magn. Reson. Spectrosc.* **1997**, *31*, 293.
[35] W. Iali, P. J. Rayner, S. B. Duckett, *Sci. Adv.* **2018**, *4*, eaao6250.
[36] K. Them, F. Ellermann, A. N. Pravdivtsev, O. G. Salnikov, I. V. Skovpin, I. V. Koptyug, R. Herges, J.-B. Hövener, *J. Am. Chem. Soc.* **2021**, *143*, 13694.
[37] E. T. V. Dyke, J. Eills, R. Picazo-Frutos, K. F. Sheberstov, Y. Hu, D. Budker, D. A. Barskiy, *Sci. Adv.* **2022**, *8*, eabp9242.
[38] P. M. Richardson, R. O. John, A. J. Parrott, P. J. Rayner, W. Iali, A. Nordon, M. E. Halse, S. B. Duckett, *Phys. Chem. Chem. Phys.* **2018**, *20*, 26362.
[39] S. L. Eriksson, J. R. Lindale, X. Li, W. S. Warren, *Sci. Adv.* **2022**, *8*, eabl3708.
[40] D. Canet, C. Aroulanda, P. Mutzenhardt, S. Aime, R. Gobetto, F. Reineri, *Concepts Magn. Reson. Part A* **2006**, *28 A*, 321.
[41] G. A. Morris, R. Freeman, *J. Am. Chem. Soc.* **1979**, *101*, 760.
[42] J. Gross, P. Costa, J. Dubacq, D. Warschawski, P. Lirsac, P. Devaux, R. Griffin, *J. Magn. Reson. Ser. B* **1995**, *106*, 187.
[43] H. Park, Q. Wang, *Chem. Sci.* **2022**, *13*, 7378.
[44] C. R. Bowers, D. P. Weitekamp, *J. Am. Chem. Soc.* **1987**, *109*, 5541.
[45] E. Y. Chekmenev, V. A. Norton, D. P. Weitekamp, P. Bhattacharya, *J. Am. Chem. Soc.* **2009**, *131*, 3164.
[46] F. Zaccagna, J. T. Grist, S. S. Deen, R. Woitek, L. M. Lechermann, M. A. McLean, B. Basu, F. A. Gallagher, *Br. J. Radiol.* **2018**, *91*, 20170688.
[47] A. Svyatova, I. V. Skovpin, N. V. Chukanov, K. V. Kovtunov, E. Y. Chekmenev, A. N. Pravdivtsev, J.-B. Hovener, I. V. Koptyug, *Chem. Eur. J.* **2019**, *25*, 8465.
[48] S. Månsson, E. Johansson, P. Magnusson, C. M. Chai, G. Hansson, J. S. Petersson, F. Ståhlberg, K. Golman, *Eur. Radiol.* **2006**, *16*, 57.
[49] J. Kurhanewicz, D. B. Vigneron, K. Brindle, E. Y. Chekmenev, A. Comment, C. H. Cunningham, R. J. DeBerardinis, G. G. Green, M. O. Leach, S. S. Rajan, R. R. Rizi, B. D. Ross, W. S. Warren, C. R. Malloy, *Neoplasia* **2011**, *13*, 81.
[50] S. Knecht, J. W. Blanchard, D. Barskiy, E. Cavallari, L. Dagys, E. VanDyke, M. Tsukanov, B. Bliemel, K. Münnemann, S. Aime, F. Reineri, M. H. Levitt, G. Buntkowsky, A. Pines, P. Blümler, D. Budker, J. Eills, *Proc. Natl. Acad. Sci. USA* **2021**, *118*, e2025383118.
[51] E. Cavallari, C. Carrera, M. Sorge, G. Bonne, A. Muchir, S. Aime, F. Reineri, *Sci. Rep.* **2018**, *8*, 8366.

Manuscript received: December 8, 2022
Version of record online: April 13, 2023